

Positive Real Synthesis Using Matrix Inequalities for Mechanical Networks: Application to Vehicle Suspension

Christakis Papageorgiou and Malcolm C. Smith, *Fellow, IEEE*

Abstract—This paper presents a procedure for the synthesis of positive real controllers based on matrix inequalities. Problems with \mathcal{H}_2 and \mathcal{H}_∞ cost are considered and the resulting bilinear matrix inequality problems are solved using local, iterative algorithms. The procedure is applied to the synthesis of passive suspensions for the optimization of certain performance measures for a quarter-car model. The characterization of the positive real constraint using matrix inequalities and the use of a new mechanical element called the inerter, permits the optimization over the entire class of positive real admittances and the realization of the resulting admittance using passive elements. The optimization results are compared with previous results obtained using optimization over fixed-structure admittances. The proposed method can reproduce the previous results and achieve better results in certain cases. Results of the experimental testing of a mechanical network involving an inerter are presented.

Index Terms—Inerter, linear matrix inequalities, mechanical device, optimization over positive real admittances, synthesis of passive mechanical networks, vehicle suspensions.

I. INTRODUCTION

POSITIVE real systems occur in many applications, for example, mechanical structures with collocated sensors and actuators, passive electrical networks (those with only resistors, inductors, and capacitors), and passive mechanical networks (those with masses, dampers, and springs). Positive real systems have motivated the design of strictly positive real compensators since the negative feedback interconnection of a positive real plant with a strictly positive real compensator is asymptotically stable.

Recently, a new mechanical network element termed the “inerter” was introduced as an alternative to the mass element for *synthesis* of mechanical networks [1]. In the context of vehicle suspensions this was exploited in [2] by optimizing standard performance measures over low-order fixed-structure admittances. The present paper considers the more general class of positive-real functions and seeks to use matrix inequalities as a tool for optimization.

Linear matrix inequalities (LMIs) [3] have emerged as a powerful paradigm and design technique for a variety of linear control problems such as \mathcal{H}_2 and \mathcal{H}_∞ synthesis. Since solving an LMI is a convex optimization problem, such formulations can be solved efficiently using interior-point algorithms. LMIs have also been successful in formulating and solving multiobjective control problems in which various performance specifications (both in the frequency and the time domain) are used for various input-output channels. It was shown in [4] that using a multiobjective formulation, the ride comfort and suspension travel could be improved for a vehicle suspension system.

The problem of synthesizing positive real compensators can be formulated using matrix inequalities since the positive real property of a system can be expressed as an LMI using the positive real lemma [3]. Considerable research has been conducted toward the synthesis of positive real controllers that achieve a level of \mathcal{H}_2 performance for the control of flexible structures. In [5], a suboptimal version of this problem is shown to be a convex optimization problem and expressed in the form of an LMI. Both the \mathcal{H}_2 and the positive real constraint are characterized using a common Lyapunov function. In [6], an iterative LMI procedure is proposed for the same problem with the difference that two separate Lyapunov functions are considered for the \mathcal{H}_2 performance and the positive real constraint. Both methods require that the order of the controller is the same as the order of the generalized plant.

In this paper, the \mathcal{H}_2 and \mathcal{H}_∞ positive real synthesis problems are formulated as bilinear matrix inequality (BMI) problems. In each case an optimization approach is used to find locally optimal solutions. The proposed algorithms allow for any order controller to be considered which is important when searching for a simple network realization of a given positive real function. It will be demonstrated using the quarter-car model that the matrix inequality approach can reproduce the results and give improvements over the previous optimization method.

II. SYNTHESIS OF ONE-PORT MECHANICAL NETWORKS

A mechanical network of pure translational type consists of mechanical elements (such as springs, masses, dampers, and levers), which are interconnected in a rigid manner. The pair of end-points of the spring and damper are called *nodes* or *terminals*. In a mechanical system, a *port* is a pair of nodes to which an equal and opposite force F is applied and which experience a relative velocity v . The force, which is a *through variable*, involves a single measurement point and requires the system to

Manuscript received January 31, 2005; revised September 6, 2005. Manuscript received in final form November 29, 2005. Recommended by Associate Editor C.-Y. Su. This work was supported in part by the Engineering and Physical Sciences Research Council, U.K.

C. Papageorgiou is with the Department of Electrical and Computer Engineering, University of Cyprus, Nicosia 1678, Cyprus (e-mail: cpapageo@ucy.ac.cy).

M. C. Smith is with the Control Group, Engineering Department, Cambridge University, Cambridge CB2 1PZ, U.K. (e-mail: mcs@eng.cam.ac.uk).

Digital Object Identifier 10.1109/TCST.2005.863663

be severed at that point to make the measurement. The velocity, which is an *across variable*, can be measured without breaking into the system and the relevant quantity is the difference of the variable between the two points. The concept of through and across variables is natural also for electrical networks and motivates the *force-current* analogy [7], which is power preserving, with the following correspondences:

$$\begin{aligned} \text{force} &\leftrightarrow \text{current} \\ \text{velocity} &\leftrightarrow \text{voltage} \\ \text{mechanical ground} &\leftrightarrow \text{electrical ground} \\ \text{kinetic energy} &\leftrightarrow \text{electrical energy} \\ \text{potential energy} &\leftrightarrow \text{magnetic energy.} \end{aligned}$$

The *impedance* $Z(s)$ of a network is defined as the ratio of the across variable to the through variable and the *admittance* $Y(s)$ is defined as the reciprocal of the impedance. Thus, mechanical admittance is the ratio of force to velocity.

A. Positive Real Functions

A mechanical one-port network with force-velocity pair (F, v) is defined to be passive if for all admissible v , F which are square integrable on $(-\infty, T]$

$$\int_{-\infty}^T F(t)v(t)dt \geq 0. \quad (1)$$

By definition, a passive network can not deliver energy to the environment. As shown in [8] and [9], the network is passive if and only if the following condition is satisfied: $Z(s)$ is analytic in $\text{Re}(s) > 0$, $Z(j\omega) + Z(j\omega)^* \geq 0$, for all ω at which $Z(j\omega)$ is finite, and any poles of $Z(s)$ on the imaginary axis or at infinity are simple and have a positive residue. Any real-rational function $Z(s)$ satisfying the above is called *positive real*. The same condition holds for admittances $Y(s)$.

The following fundamental theorem is used in electrical circuit synthesis of positive real impedances and admittances.

Theorem 2.1 [9], [10]: Consider any real-rational function $Z(s)$, $(Y(s))$ which is positive real. There exists a one-port electrical network whose impedance (admittance) equals $Z(s)$ ($Y(s)$) which consists of a finite interconnection of inductors, resistors, and capacitors.

B. The Inerter

It was pointed out in [1] that Theorem 2.1 cannot be applied directly to the synthesis of mechanical networks because of the fact that the mass element is analogous to a *grounded capacitor*. Thus, the mechanical analog of an electrical network with ungrounded capacitors can not be realized with the use of springs, dampers, and masses. This imposes a restriction on the class of passive mechanical impedances which can be physically realized. This restriction is lifted by defining a new mechanical element, the *inertor*, which is the mechanical analog of the ungrounded capacitor.

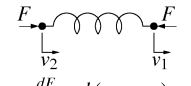
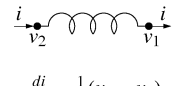
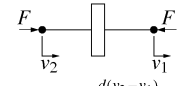
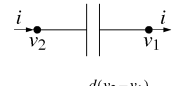
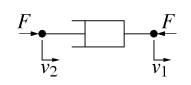
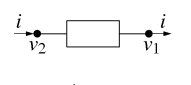
Mechanical	Electrical
 $Y(s) = \frac{k}{s}$ $\frac{dF}{dt} = k(v_2 - v_1)$ spring	 $Y(s) = \frac{1}{Ls}$ $\frac{di}{dt} = \frac{1}{L}(v_2 - v_1)$ inductor
 $Y(s) = bs$ $F = b \frac{d(v_2 - v_1)}{dt}$ inerter	 $Y(s) = Cs$ $i = C \frac{d(v_2 - v_1)}{dt}$ capacitor
 $Y(s) = c$ $F = c(v_2 - v_1)$ damper	 $Y(s) = \frac{1}{R}$ $i = \frac{1}{R}(v_2 - v_1)$ resistor

Fig. 1. Circuit symbols and correspondences with defining equations and admittance $Y(s)$.

Definition 2.1 (Inerter [1]): The (ideal) inerter is a mechanical two-terminal device with the property that the equal and opposite force applied at the nodes is proportional to the relative acceleration between the nodes, i.e., $F = b(\ddot{v}_2 - \ddot{v}_1)$ where v_1, v_2 are the velocities of the two terminals and b is a constant of proportionality called the *inertance*, which has units of kilograms.

The element correspondences in the force-current analogy with the inerter replacing the mass element are shown in Fig. 1.

Prototype inerters have been built at Cambridge University Engineering Department (CUED) using the following: 1) a plunger sliding in a cylinder which drives a flywheel through a rack, pinion and gears [2] and 2) a ball-screw mechanism. Experiments using the latter device are described in Section VIII of the present paper.

C. The Control Synthesis Paradigm

In [2], mechanical networks comprising springs, dampers, and inerters were studied for use in passive suspensions for both quarter-car and full-car vehicle models. Performance advantages were found for ride comfort and handling compared to conventional passive suspension struts. The approach in [2] was to consider various fixed-structure admittances which contained at most one inerter and one damper. The parameter values of the components were tuned in order to optimize the various performance measures. This method addresses only a small part of the class of positive real admittances that can be physically realized. In order to be able to synthesize admittances over the whole class of positive real functions, we use a control synthesis paradigm along with a state-space characterization of positive realness. The search for positive real admittances is formulated as a search for positive real “controllers” $K(s)$ as shown in Fig. 2. The characterization of positive realness of the controller is achieved with the following result. This approach requires the order of the controller to be specified in the optimization procedure.

Lemma 2.2 (Positive Real Lemma [3]): Given that

$$K(s) = \left[\begin{array}{c|c} A_k & B_k \\ \hline C_k & D_k \end{array} \right] = C_k(sI - A_k)^{-1}B_k + D_k \quad (2)$$

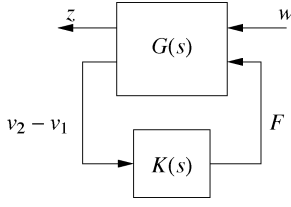


Fig. 2. Control synthesis paradigm applied for the synthesis of a positive real admittance $K(s)$.

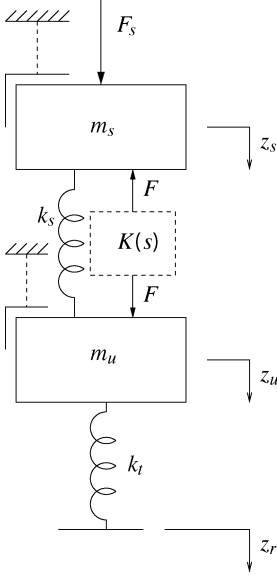


Fig. 3. Quarter-car vehicle model with predetermined static stiffness.

then $K(s)$ is positive real if and only if there exists $P_k > 0$ that satisfies the LMI

$$\begin{bmatrix} A_k^T P_k + P_k A_k & P_k B_k - C_k^T \\ B_k^T P_k - C_k & -D_k^T - D_k \end{bmatrix} \leq 0. \quad (3)$$

III. VEHICLE SUSPENSIONS

A. The Quarter-Car Model

The quarter-car model presented in Fig. 3 is the simplest model to consider for suspension design. It consists of the sprung mass m_s , the unsprung mass m_u , and a tyre with spring stiffness k_t . The suspension strut provides an equal and opposite force on the sprung and unsprung masses and is assumed to be a passive mechanical admittance $Y(s) = K(s) + (k_s/s)$, where $K(s)$ is positive real and has no pole at $s = 0$. In this paper, we fix the parameters of the quarter-car model as $m_s = 250$ kg, $m_u = 35$ kg, $k_t = 150$ kN/m.

B. Performance Measures

There are a number of practical design requirements for a suspension system, such as passenger comfort, handling, tyre normal loads, and limits on suspension travel, which require careful optimization. In the quarter-car model these can be translated approximately into specifications on the transfer functions from the disturbance signals F_s and z_r to the signals z_s and z_u . The performance measures used in this paper are discussed

in detail in [2]. The first two assume a standard rational power spectrum for the road disturbances, while the third relates to the effect of loads on the sprung mass.

For the ride comfort we use the root-mean-square (rms) body vertical acceleration in response to road disturbances, denoted by J_1 , which is equal to

$$J_1 = 2\pi(V\kappa)^{\frac{1}{2}} \|sT_{\hat{z}_r \rightarrow \hat{z}_s}\|_2 \quad (4)$$

where V is the speed of the car, κ is the road roughness parameter, $T_{\hat{z}_r \rightarrow \hat{z}_s}$ denotes the transfer function from the road disturbance z_r to the displacement of the sprung mass z_s , and $\|\cdot\|_2$ is the standard \mathcal{H}_2 norm.

To characterize road holding we use the rms dynamic tyre load in response to road disturbances, denoted by J_3 , which is equal to

$$J_3 = 2\pi(V\kappa)^{\frac{1}{2}} \left\| \frac{1}{s} T_{\hat{z}_r \rightarrow k_t(\hat{z}_u - \hat{z}_r)} \right\|_2. \quad (5)$$

Another factor to be considered is the ability of the suspension to withstand external loads on the sprung mass, e.g., those loads induced by braking, accelerating, and cornering. The following measure is used for this purpose:

$$J_5 = \|T_{\hat{F}_s \rightarrow \hat{z}_s}\|_{\infty} \quad (6)$$

where $\|\cdot\|_{\infty}$ represents the \mathcal{H}_{∞} -norm. We will attempt to minimize each performance measure on its own over positive real admittances $Y(s)$ of fixed degree and compare the results with those obtained in [2].

C. The Quarter-Car Model as a Linear Fractional Transformation for the Optimization of J_1 and J_5

Since the performance measures are expressed as either \mathcal{H}_2 or \mathcal{H}_{∞} norms of certain transfer functions, it is proposed to formulate the suspension design problem as a standard \mathcal{H}_2 or \mathcal{H}_{∞} controller synthesis problem. This requires that the quarter-car model is written as a linear fractional transformation (LFT) with respect to the unknown, positive real admittance $K(s)$. The interconnection used for the derivation of the generalized, quarter-car plant is given in Fig. 3. We require that the static stiffness of the suspension is determined *a priori* and is given by k_s . The equations of motion are given by

$$\ddot{z}_s = \frac{F_s}{m_s} - \frac{F}{m_s} - \frac{k_s}{m_s} z_s + \frac{k_s}{m_s} z_u \quad (7)$$

$$\ddot{z}_u = \frac{F}{m_u} + \frac{k_s}{m_u} z_s - \frac{k_s}{m_u} z_u + \frac{k_t}{m_u} z_r - \frac{k_t}{m_u} z_u \quad (8)$$

$$\hat{F} = K(s)(s\hat{z}_s - s\hat{z}_u). \quad (9)$$

The external input of the generalized plant is $w = [F_s, z_r]^T$, while the performance output is given by $z = [\dot{z}_s, z_s]^T$. Writing the above equations in state-space form with the state vector given by $x = [\dot{z}_s, z_s, \dot{z}_u, z_u]^T$ results in the quarter-car, generalized plant

$$\dot{x} = Ax + B \begin{bmatrix} w \\ F \end{bmatrix}, \quad \begin{bmatrix} z \\ \dot{z}_s - \dot{z}_u \end{bmatrix} = Cx \quad (10)$$

where

$$A = \begin{bmatrix} 0 & -\frac{k_s}{m_s} & 0 & \frac{k_s}{m_s} \\ 1 & 0 & 0 & 0 \\ 0 & \frac{k_s}{m_u} & 0 & -\frac{k_s+k_t}{m_u} \\ 0 & 0 & 1 & 0 \end{bmatrix}$$

$$B = \begin{bmatrix} \frac{1}{m_s} & 0 & -\frac{1}{m_s} \\ 0 & 0 & 0 \\ 0 & \frac{k_t}{m_u} & \frac{1}{m_u} \\ 0 & 0 & 0 \end{bmatrix}$$

$$C = \begin{bmatrix} 1 & 0 & 0 & 0 \\ 0 & 1 & 0 & 0 \\ 1 & 0 & -1 & 0 \end{bmatrix}.$$

Let B_1, B_2, B_3 be the respective columns of B , and let C_1, C_2, C_3 be the respective rows of C . Since the static stiffness is determined *ita priori*, the admittance $K(s)$ must have zero static stiffness, hence, it may not contain an integrator. This is in fact ensured by the structure of the generalized plant. The transfer function from F to $\dot{z}_s - \dot{z}_u$ is given by

$$T_{F \rightarrow (\dot{z}_s - \dot{z}_u)} = -\frac{s((m_u + m_s)s^2 + k_t)}{m_u m_s s^4 + s^2(m_u k_s + k_s m_s + k_t m_s) + k_t k_s}.$$

Therefore, a “stabilizing controller” $K(s)$ cannot have an integrator because it will cause a right-half plane (RHP) pole-zero cancellation [11, Sec. 12.1].

IV. OPTIMIZATION OF J_1

The generalized plant for the J_1 optimization is formed by considering z_r as the external disturbance and \dot{z}_s as the performance output. The objective is to find a positive real $K(s)$ so that $\|T_{\dot{z}_r \rightarrow s\dot{z}_s}\|_2$ is minimized. From (10), the observable and controllable representation of the J_1 generalized plant is given by

$$\dot{x} = Ax + B_2 z_r + B_3 F \quad (11)$$

$$\dot{z}_s = C_1 x, \quad \dot{z}_s - \dot{z}_u = C_3 x. \quad (12)$$

Given a controller $K(s)$ of order n_k , with state-space representation as in (2), let the state-space representation of the closed-loop system resulting from the interconnection of the generalized plant and the controller be given by

$$\begin{bmatrix} \dot{x} \\ \dot{x}_k \\ \dot{z}_s \end{bmatrix} = \begin{bmatrix} A_{cl} & B_{cl} \\ C_{cl} & 0 \end{bmatrix} \begin{bmatrix} x \\ x_k \\ z_r \end{bmatrix}. \quad (13)$$

Theorem 4.1: There exists a positive real controller $K(s)$ of order n_k such that $\|T_{\dot{z}_r \rightarrow s\dot{z}_s}\|_2 < v$ and A_{cl} is stable, if and only if the following problem is feasible for some $X_{cl} > 0, X_k > 0, Q, v^2$ and A_k, B_k, C_k, D_k of compatible dimensions:

$$\begin{bmatrix} A_{cl}^T X_{cl} + X_{cl} A_{cl} & X_{cl} B_{cl} \\ B_{cl}^T X_{cl} & -I \end{bmatrix} < 0, \quad \begin{bmatrix} X_{cl} & C_{cl}^T \\ C_{cl} & Q \end{bmatrix} > 0$$

$$\text{tr}(Q) < v^2, \quad \begin{bmatrix} A_k^T X_k + X_k A_k & X_k B_k - C_k^T \\ B_k^T X_k - C_k & -D_k^T - D_k \end{bmatrix} < 0.$$

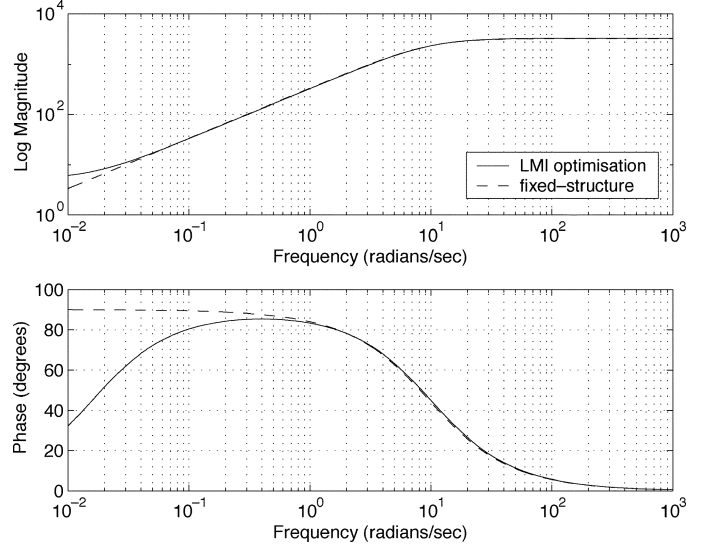


Fig. 4. Comparison of first-order admittances $K(s)$ for the quarter-car model for $k_s = 60$ kN/m.

The first three LMIs are necessary and sufficient conditions for the existence of a stabilizing controller that achieves an upper bound of v on the \mathcal{H}_2 -norm [12]. The fourth LMI further restricts the controller to be positive real. Without the positive real constraint, the \mathcal{H}_2 -synthesis problem can be formulated as an LMI problem as shown in [12]. With the positive real constraint it is not obvious how to do so, hence, an iterative optimization method is employed to solve the BMI problem locally. The method, which is described in [13], is to linearize the BMI using a first-order perturbation approximation, and then iteratively compute a perturbation that “slightly” improves the controller performance by solving an LMI problem. The proposed scheme is already implemented in YALMIP [14], which is a MATLAB toolbox for rapid prototyping of optimization problems. A feasible starting point must be given to the algorithm.

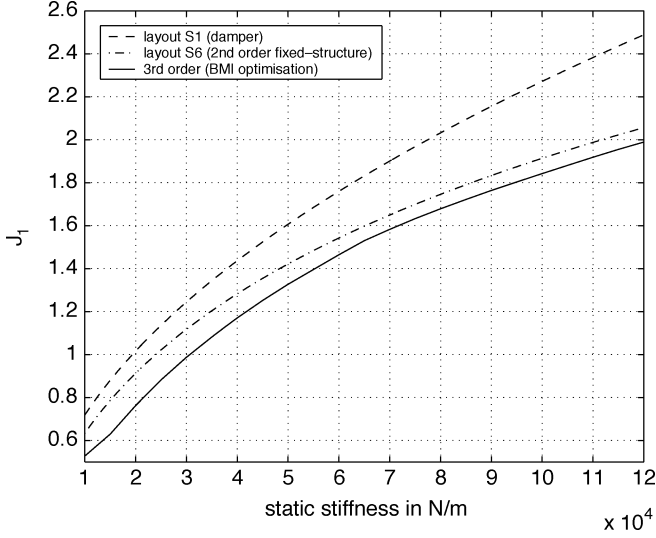
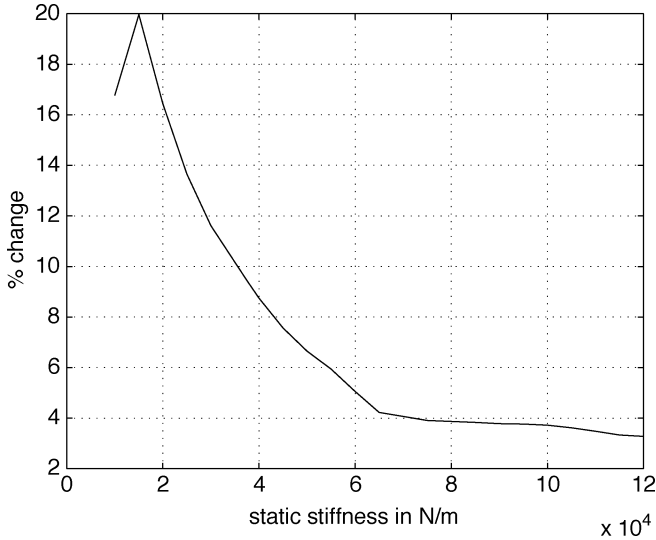
A. J_1 Optimization Results

There are two issues to be investigated regarding the proposed synthesis method. The first is whether it can reproduce the results of the fixed-structure optimization and the second, whether it can give improved levels of performance exploiting the optimization over the entire class of positive real admittances.

An example is presented that demonstrates that the proposed method is successful in reproducing the fixed-structure optimization results. The quarter-car model is considered with static stiffness $k_s = 60$ kN/m. The fixed-structure admittance proposed in [2] is a damper in series with an inerter, i.e., $K(s) = bs/(c + bs)$, which achieves a value of $J_1 = 1.5851$ for $c = 3224$ Ns/m and $b = 334$ kg. The admittance $K(s)$ calculated by YALMIP is given by

$$K(s) = \frac{3276s + 52}{s + 10} = 5.2 + \left(\frac{1}{3271} + \frac{1}{327.1s} \right)^{-1} \quad (14)$$

and achieves $J_1 = 1.5855$. A comparison of the two admittances is shown in Fig. 4. The YALMIP admittance cannot ex-


 Fig. 5. Improvement in J_1 when using higher order admittances.

 Fig. 6. Percentage improvement in J_1 when $K(s)$ is third-order.

actly match the fixed-structure admittance because it can only optimize over the class of strictly positive real controllers which implies $\text{Re}(K(j\omega)) > 0$.

Apart from being able to approximately achieve the fixed-structure admittances suggested in [2] it is useful to know whether J_1 can be reduced further by optimizing over higher order admittances. The highest order admittance used in [2] was of second order. The best results obtained so far with third-order admittances are presented in Fig. 5 as a function of the static stiffness of the suspension, along with previous results related to fixed-structure admittances. The “best” fixed-structure admittance found in [2] is a parallel connection of a damper and centering spring in series with a parallel connection of an inerter and centering spring and was given the name layout S6. The percentage improvement is calculated with respect to the values of J_1 achieved by the S6 fixed-structure admittance. The results are shown in Fig. 6. The optimization algorithm

was run for values of static stiffness in the range 10–120 kN/m at a spacing of 5 kN/m.

V. OPTIMIZATION OF J_3

A. Generalized Plant for the Optimization of J_3

The performance output corresponding to J_3 is given by $\int k_t(z_u - z_r)$. This is implemented by adding an integrator on $k_t(z_u - z_r)$, thus creating one more state for the generalized plant. The generalized plant for the optimization of J_3 is given by

$$\begin{bmatrix} \ddot{z}_s \\ \dot{z}_s \\ \ddot{z}_u \\ \dot{z}_u \\ \dot{x}_1 \end{bmatrix} = \begin{bmatrix} 0 & -\frac{k_s}{m_s} & 0 & \frac{k_s}{m_s} & 0 \\ 1 & 0 & 0 & 0 & 0 \\ 0 & \frac{k_s}{m_u} & 0 & -\frac{k_s+k_t}{m_u} & 0 \\ 0 & 0 & 1 & 0 & 0 \\ 0 & 0 & 0 & k_t & 0 \end{bmatrix} \begin{bmatrix} \dot{z}_s \\ z_s \\ \dot{z}_u \\ z_u \\ x_1 \end{bmatrix} + \begin{bmatrix} 0 & -\frac{1}{m_s} \\ 0 & 0 \\ \frac{k_t}{m_u} & \frac{1}{m_u} \\ 0 & 0 \\ -k_t & 0 \end{bmatrix} \begin{bmatrix} z_r \\ F \end{bmatrix} \quad (15)$$

$$\begin{bmatrix} \int k_t(z_u - z_r) \\ \dot{z}_s - \dot{z}_u \end{bmatrix} = \begin{bmatrix} 0 & 0 & 0 & 0 & 1 \\ 1 & 0 & -1 & 0 & 0 \end{bmatrix} \begin{bmatrix} \dot{z}_s \\ z_s \\ \dot{z}_u \\ z_u \\ x_1 \end{bmatrix} + \begin{bmatrix} 0 & 0 \\ 0 & 0 \end{bmatrix} \begin{bmatrix} z_r \\ F \end{bmatrix}. \quad (16)$$

The addition of the extra integrator creates problems since the added state is uncontrollable. Consider the similarity transformation given by

$$\begin{bmatrix} \dot{z}_s \\ z_s \\ \dot{z}_u \\ z_u \\ x_n \end{bmatrix} = \begin{bmatrix} 1 & 0 & 0 & 0 & 0 \\ 0 & 1 & 0 & 0 & 0 \\ 0 & 0 & 1 & 0 & 0 \\ 0 & 0 & 0 & 1 & 0 \\ m_s & 0 & m_u & 0 & 1 \end{bmatrix} \begin{bmatrix} \dot{z}_s \\ z_s \\ \dot{z}_u \\ z_u \\ x_1 \end{bmatrix}. \quad (17)$$

The transformed system equations are

$$\begin{bmatrix} \ddot{z}_s \\ \dot{z}_s \\ \ddot{z}_u \\ \dot{z}_u \\ \dot{x}_n \end{bmatrix} = \begin{bmatrix} 0 & -\frac{k_s}{m_s} & 0 & \frac{k_s}{m_s} & 0 \\ 1 & 0 & 0 & 0 & 0 \\ 0 & \frac{k_s}{m_u} & 0 & -\frac{k_s+k_t}{m_u} & 0 \\ 0 & 0 & 1 & 0 & 0 \\ 0 & 0 & 0 & 0 & 0 \end{bmatrix} \begin{bmatrix} \dot{z}_s \\ z_s \\ \dot{z}_u \\ z_u \\ x_n \end{bmatrix} + \begin{bmatrix} 0 & -\frac{1}{m_s} \\ 0 & 0 \\ \frac{k_t}{m_u} & \frac{1}{m_u} \\ 0 & 0 \\ 0 & 0 \end{bmatrix} \begin{bmatrix} z_r \\ F \end{bmatrix} \quad (18)$$

$$\begin{bmatrix} \int k_t(z_u - z_r) \\ \dot{z}_s - \dot{z}_u \end{bmatrix} = \begin{bmatrix} -m_s & 0 & -m_u & 0 & 1 \\ 1 & 0 & -1 & 0 & 0 \end{bmatrix} \begin{bmatrix} \dot{z}_s \\ z_s \\ \dot{z}_u \\ z_u \\ x_n \end{bmatrix} + \begin{bmatrix} 0 & 0 \\ 0 & 0 \end{bmatrix} \begin{bmatrix} z_r \\ F \end{bmatrix}. \quad (19)$$

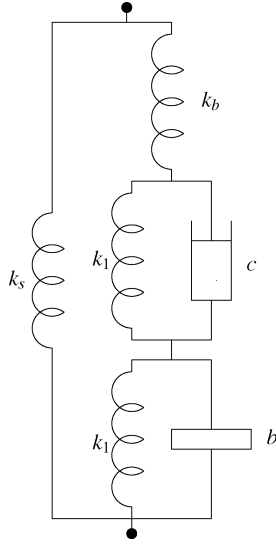


Fig. 7. S7 suspension layout proposed in [2].

It is evident that the state x_n is uncontrollable so it can be removed. Furthermore, the output equation

$$\int k_t(z_u - z_r) = -m_s \dot{z}_s - m_u \dot{z}_u \quad (20)$$

is divided by k_t in order to make the state-space matrices more well-conditioned resulting in

$$\int (z_u - z_r) = -\frac{m_s}{k_t} \dot{z}_s - \frac{m_u}{k_t} \dot{z}_u. \quad (21)$$

The performance measure is now equal to

$$J_3 = 2\pi(V\kappa)^{\frac{1}{2}} k_t \left\| T_{\hat{z}_r \rightarrow \int(z_u - \hat{z}_r)} \right\|_2. \quad (22)$$

The generalized plant for the J_3 optimization is finally given by

$$P_{J_3}(s) = \left[\begin{array}{c|c} \begin{bmatrix} 0 & -\frac{k_s}{m_s} & 0 & \frac{k_s}{m_s} \\ 1 & 0 & 0 & 0 \\ 0 & \frac{k_s}{m_u} & 0 & -\frac{k_s+k_t}{m_u} \\ 0 & \frac{m_s}{m_u} & 1 & 0 \end{bmatrix} & \begin{bmatrix} 0 & -\frac{1}{m_s} \\ 0 & 0 \\ \frac{k_t}{m_u} & \frac{1}{m_u} \\ 0 & 0 \end{bmatrix} \\ \hline \begin{bmatrix} -\frac{m_s}{k_t} & 0 & -\frac{m_u}{k_t} & 0 \\ 1 & 0 & -1 & 0 \end{bmatrix} & \begin{bmatrix} 0 & 0 \\ 0 & 0 \end{bmatrix} \end{array} \right]. \quad (23)$$

The J_3 optimization problem is similar to the J_1 optimization problem, i.e., a positive real controller $K(s)$ is sought to minimize the \mathcal{H}_2 norm of the closed-loop transfer function. A theorem can be written down which is directly analogous to Theorem 4.1 to give a necessary and sufficient condition for the achievement of a certain performance level. Again, this characterization is in the form of a BMI which can be solved locally using the iterative algorithm implemented in YALMIP.

B. J_3 Optimization Results

The optimization of the J_3 measure was attempted in [2] over fixed structure suspensions. The maximum order of the considered fixed structure admittances was three. The third-order suspension is referred to as S7 and is shown in Fig. 7. The

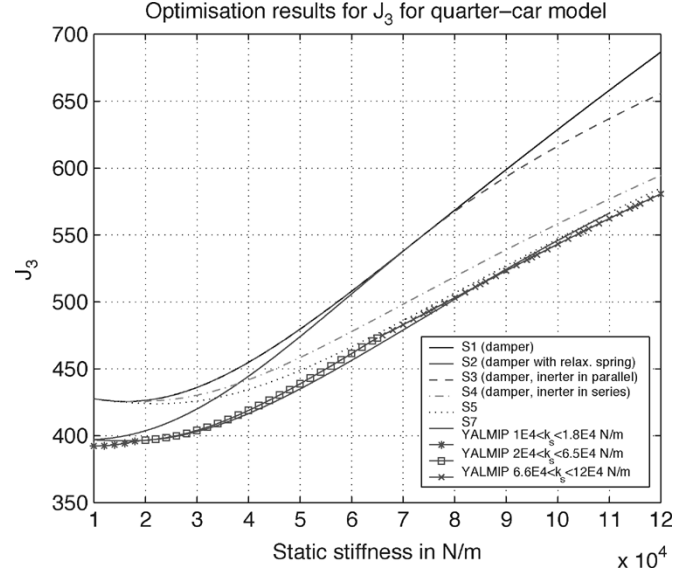


Fig. 8. Comparison of YALMIP optimization results with fixed-structure optimization results for J_3 .

fixed-structure second-order layout is referred to as S5 and is the same as S7 with the relaxation spring k_b removed.

The iterative algorithm implemented in YALMIP was used to optimize J_3 over general second-order admittances in order to investigate whether J_3 can be improved further. The optimization was performed for k_s ranging from 10 to 120 kN/m in steps of 2 kN/m. The comparison of the optimization results obtained with YALMIP with those obtained by fixed-structure optimization are presented in Fig. 8. The results exhibit three distinct curves suggesting that the structure of the suspension changes as the static stiffness varies. At low and high stiffness, the YALMIP second-order admittance can do better than both the second-order S5 layout and the third-order S7 layout. An encouraging feature of the optimization algorithm is that it automatically finds the change in the structure of the admittance as the static stiffness varies in order to obtain the minimum value of J_3 . It is of interest to investigate the structure of the suspensions obtained with YALMIP and understand how they differ from the fixed-structure suspensions.

1) *The Suspensions Corresponding to the Low Static Stiffness Range* ($10 \text{ kN/m} < k_s < 18 \text{ kN/m}$): As a representative of this class of admittances we consider the admittance of the suspension for $k_s = 12 \text{ kN/m}$. The admittance is given by

$$K(s) = \frac{32.566(s + 3955)(s + 183.43)}{s^2 + 133.71s + 12545} \quad (24)$$

and it achieves a value of $J_3 = 392.5$. A simpler admittance is constructed by canceling the term $(s + 3955)$ and by modifying the term $(s + 183.43)$ sufficiently to maintain the positive real character of the new admittance. The new admittance is given by

$$K_{ap}(s) = \frac{32.566 \times 3955 \times 183.43(s + 133)}{s^2 + 133.71s + 12545}. \quad (25)$$

Its frequency response is compared with the frequency response of $K(s)$ and with the frequency response of the fixed-structure

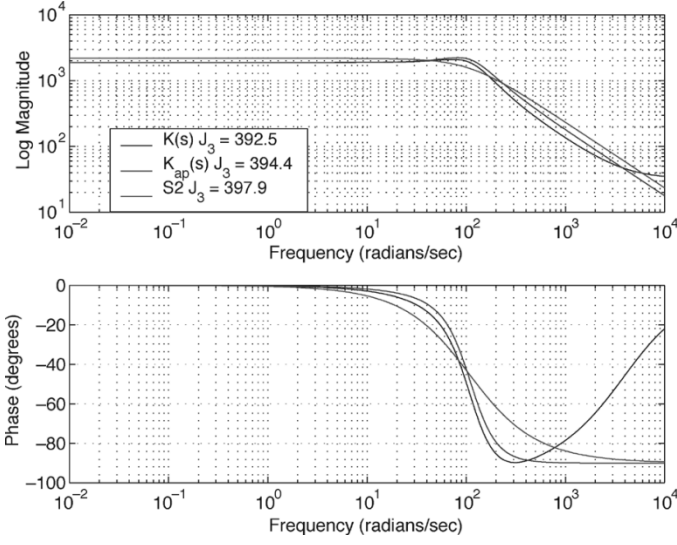


Fig. 9. Comparison of the original and approximate admittances at $k_s = 12$ kN/m.

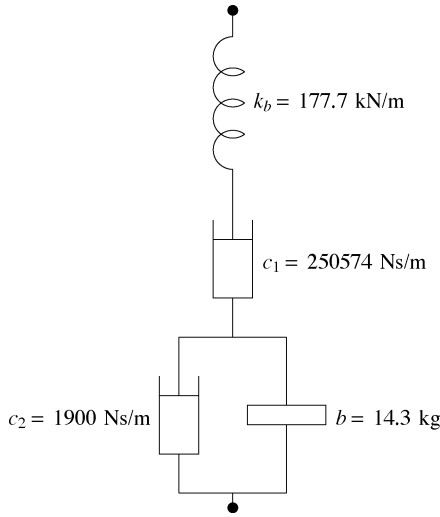


Fig. 10. Suspension layout corresponding to the admittance $K_{ap}(s)$.

admittance S2 (damper in series with relaxation spring, see [2]) in Fig. 9. The approximate admittance achieves $J_3 = 394.4$ and its realization is given in Fig. 10. If we remove the small inductance in the realization of Fig. 10, the suspension layout becomes the same as the S2 layout but with slightly different values for k_b and c from the ones obtained in [2]. Therefore, it seems that the 1.5% improvement in J_3 does not justify the extra complexity of the realization in Fig. 10 over the S2 layout and the unrealistic damper rate of c_1 (although a very large damper rate implies a short circuit and, thus, it can be neglected).

2) *The Suspensions Corresponding to the Intermediate Static Stiffness Range* (20 kN/m $< k_s < 65$ kN/m): As a representative of this class of admittances we consider the admittance of the suspension for $k_s = 50$ kN/m. The admittance is given by

$$K(s) = \frac{1.3(s + 222633)(s + 0.148 \times 10^3)}{(s + 90.3)(s + 10.8)} \quad (26)$$

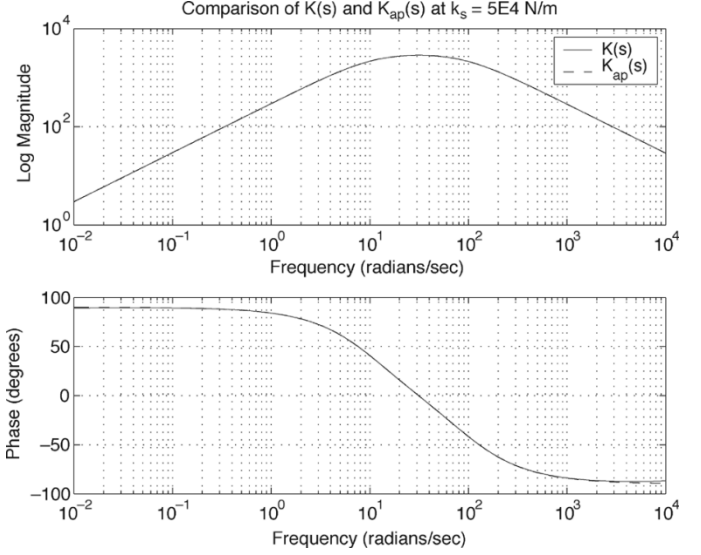


Fig. 11. Comparison of the original and approximate admittances for $k_s = 50$ kN/m.

and it achieves a value of $J_3 = 438.8$. A simpler admittance is constructed by canceling the term $(s + 222633)$ and by approximating the term $(s + 0.148 \times 10^3)$ with s . The approximate admittance is given by

$$K_{ap}(s) = \frac{288510s}{(s + 90.3)(s + 10.8)} \quad (27)$$

and it achieves $J_3 = 438.8$, i.e., there is practically no degradation in J_3 . The comparison of the frequency responses of the original admittance $K(s)$ with $K_{ap}(s)$ is shown in Fig. 11. A realization of $K_{ap}(s)$ is constructed by noting that,

$$K_{ap}(s) = \left(\frac{1}{\frac{288510}{s}} + \frac{1}{2857} + \frac{1}{297s} \right)^{-1} \quad (28)$$

It is obvious that $K_{ap}(s)$ is the admittance of the network consisting of an inerter in series with a damper in series with a spring shown in Fig. 12. Note that the layout S7 would be the same as the layout of Fig. 12 if we include centering springs in parallel with the damper and the inerter.

3) *The Suspensions Corresponding to the High Static Stiffness Range* (66 kN/m $< k_s < 120$ kN/m): As a representative of this class of admittances we consider the admittance of the suspension for $k_s = 90$ kN/m. The admittance is given by

$$K(s) = \frac{3306.1(s + 8.08)(s + 0.5564)}{s^2 + 12.1s + 152.12} \quad (29)$$

and achieves $J_3 = 523.3$. A simpler admittance is constructed by making the term $(s + 0.5564)$ equal to s and by modifying the remaining terms so that the positive real property is preserved. The approximate admittance is given by

$$K_{ap}(s) = \frac{3306.1s(s + 13)}{s^2 + 13s + 152.12} \quad (30)$$

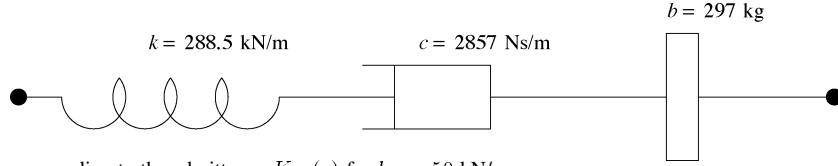


Fig. 12. Suspension layout corresponding to the admittance $K_{ap}(s)$ for $k_s = 50$ kN/m.

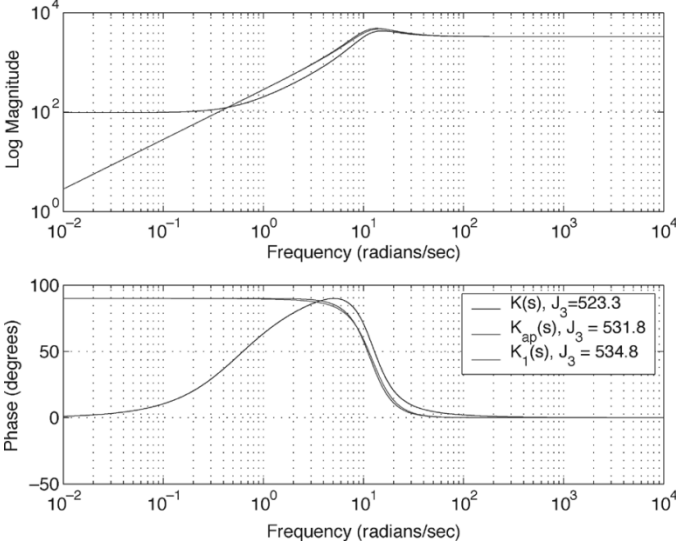


Fig. 13. Comparison of $K(s)$ and $K_{ap}(s)$ at $k_s = 90$ kN/m.

and achieves $J_3 = 531.8$, i.e., there is 1.6% degradation in J_3 . A comparison of the frequency responses between $K(s)$ and $K_{ap}(s)$ is shown in Fig. 13. A realization for the admittance $K_{ap}(s)$ is found by noting that

$$\begin{aligned} K_{ap}(s) &= 3306.1 \left(\frac{11.7}{s} + \frac{13s+16.88}{13s+169} \right)^{-1} \\ &= 3306.1 \left(\frac{11.7}{s} + \left(1 + \frac{152.12}{13s+16.88} \right)^{-1} \right)^{-1} \\ &= \left(\frac{1}{282.6s} + \left(3306.1 + \left(\frac{1}{38686} + \frac{1}{29794} \right)^{-1} \right)^{-1} \right)^{-1}. \end{aligned} \quad (31)$$

The mechanical network corresponding to the admittance in (31) is shown in Fig. 14. Taking into account that a large value of damper rate is a short circuit, we remove the large damper of $c = 29794$ Ns/m and investigate the remaining admittance ($K_1(s)$). The change in the frequency response from that of $K_{ap}(s)$ is hardly noticeable (see Fig. 13) but J_3 deteriorates by 0.6% to a value of 534.8.

As seen in this section, it is frequently the case that an admittance obtained from the optimization algorithm may be approximated by a positive real function of the same or lower order to permit a simpler realization, while incurring only a minimal degradation in performance. This has been carried out here on a case-by-case basis without seeking a systematic method to achieve this.

VI. OPTIMIZATION OF J_5

The generalized plant for the J_5 optimization is formed by considering F_s as the external disturbance and z_s as the performance output. The objective is to find a positive real $K(s)$ so that $J_5 = \|T_{\hat{F}_s \rightarrow \hat{z}_s}\|_\infty$ is minimized. Here it is advantageous to allow the admittance $K(s)$ to be either proper or nonproper. The proper admittance is given by (2) and the nonproper one is given by

$$K(s) = C_k(sI - A_k)^{-1}B_k + D_k + sE_k \quad (32)$$

with $E_k > 0$ in order to satisfy positive realness along with the LMI condition (3). The term sE_k represents an inerter with inertance E_k in parallel with the proper admittance.

A. Optimization Over Proper Controllers

From (10), the observable and controllable representation of the J_5 generalized plant is

$$\dot{x} = Ax + B_1 F_s + B_3 F \quad (33)$$

$$z_s = C_2 x, \quad \dot{z}_s - \dot{z}_u = C_3 x. \quad (34)$$

Given a controller $K(s)$ of order n_k , with state-space representation as in (2), let the state-space representation of the closed-loop system resulting from the interconnection of the generalized plant and the controller be denoted by

$$\begin{bmatrix} \dot{x} \\ \dot{x}_k \\ \dot{z}_s \end{bmatrix} = \begin{bmatrix} A_{cl} & B_{cl} \\ C_{cl} & D_{cl} \end{bmatrix} \begin{bmatrix} x \\ x_k \\ F_s \end{bmatrix}. \quad (35)$$

Theorem 6.1: There exists a positive real controller $K(s)$ of order n_k such that $J_5 = \|T_{\hat{F}_s \rightarrow \hat{z}_s}\|_\infty < \gamma$ and A_{cl} is stable, if and only if, the following problem is feasible for some $X_{cl} > 0$, $X_k > 0$, $\gamma > 0$ and A_k, B_k, C_k, D_k of compatible dimensions

$$M < 0, \quad \begin{bmatrix} A_k^T X_k + X_k A_k & X_k B_k - C_k^T \\ B_k^T X_k - C_k^T & -D_k^T - D_k \end{bmatrix} < 0 \quad (36)$$

where $X_{cl} := \begin{bmatrix} X_{11} & X_{12} \\ X_{12}^T & X_{22} \end{bmatrix}$ and M is a symmetric matrix with

$$M_{11} = X_{11}A + ()^T + X_{11}B_3D_kC_3 + ()^T + X_{12}B_kC_3 + ()^T$$

$$M_{12} = X_{11}B_3C_k + X_{12}A_k + A^T X_{12} + C_3^T D_k^T B_3^T X_{12} + C_3^T B_k^T X_{22}$$

$$M_{13} = X_{11}B_1, \quad M_{14} = C_2^T, \quad M_{23} = X_{12}^T B_1$$

$$M_{22} = X_{22}A_k + ()^T + X_{12}^T B_3C_k + ()^T$$

$$M_{24} = 0_{n_k \times 1}, \quad M_{34} = 0, \quad M_{33} = M_{44} = -\gamma I$$

where $()^T$ denotes the transpose of the preceding matrix.

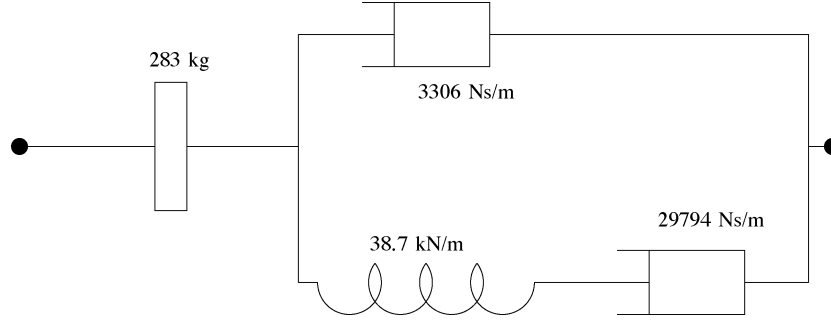


Fig. 14. Suspension layout corresponding to the admittance $K_{ap}(s)$ for $k_s = 90$ kN/m.

The matrix inequality $M < 0$ results by applying the Bounded Real Lemma on the closed-loop system of (35), which is a necessary and sufficient condition for the existence of a stabilizing controller that achieves an upper bound on the \mathcal{H}_∞ -norm. In the absence of the positive real constraint, the search for a stabilizing controller of order $n_k = n$ that minimizes the closed-loop \mathcal{H}_∞ norm was formulated as a convex optimization problem in [15]. With the additional positive real constraint, it is not obvious how to formulate the problem as a convex problem.

The problem of Theorem 6.1 is a BMI and an iterative algorithm is proposed to solve the problem locally about a feasible starting point. The idea is to fix a subset of the decision variables so that the matrix inequality is linear with respect to the remaining decision variables and thus can be solved efficiently. The steps for the algorithm are described below.

- 1) Decide on the static stiffness k_s of the suspension and on the order of the controller n_k . Give an initial controller (A_k, B_k, C_k, D_k) which is positive real (as well as stabilizing).
- 2) For the given controller, minimize γ over the Lyapunov matrices X_{cl} and X_k that are associated with the \mathcal{H}_∞ bound and the positive real condition, respectively.
- 3) Fix X_{cl} and X_k according to the values of the previous step. Minimize γ over the controller matrices, using as an initial starting point, the previous controller matrices and the value of γ from the previous step.
- 4) Unless γ satisfies some stopping criterion, go to step 2.

Note that there is a theoretical minimum of J_5 given by $J_{5\min} = k_s^{-1} + k_t^{-1}$ which is equal to $T_{\hat{F}_s \rightarrow \hat{z}_s}(0)$.

B. Optimization Over Nonproper Controllers

The nonproper admittance (32) can be represented in ordinary state-space form by introducing a second measurement equal to the acceleration signal $(\ddot{z}_s - \ddot{z}_u)$ as follows:

$$\dot{x}_k = A_k x_k + [B_k \quad 0_{n_k \times 1}] \begin{bmatrix} \dot{z}_s - \dot{z}_u \\ \ddot{z}_s - \ddot{z}_u \end{bmatrix}, \quad x_k \in \mathbb{R}^{n_k} \quad (37)$$

$$F = C_k x_k + [D_k \quad E_k] \begin{bmatrix} \dot{z}_s - \dot{z}_u \\ \ddot{z}_s - \ddot{z}_u \end{bmatrix}. \quad (38)$$

The J_5 generalized plant equations are augmented by the acceleration measurement output to give the following equation:

$$\begin{bmatrix} \dot{z}_s - \dot{z}_u \\ \ddot{z}_s - \ddot{z}_u \end{bmatrix} = \begin{bmatrix} C_3 \\ C_4 \end{bmatrix} x + \begin{bmatrix} 0 \\ D_1 \end{bmatrix} F_s + \begin{bmatrix} 0 \\ D_2 \end{bmatrix} F \quad (39)$$

where

$$C_4 = \begin{bmatrix} 0 & -\frac{k_s}{m_s} - \frac{k_s}{m_u} & 0 & \frac{k_s}{m_s} + \frac{k_s + k_t}{m_u} \end{bmatrix} \quad (40)$$

$$D_1 = \frac{1}{m_s}$$

$$D_2 = -\frac{1}{m_s} - \frac{1}{m_u}. \quad (41)$$

With the change of variable

$$Z_k = (1 - E_k D_2)^{-1} \Leftrightarrow E_k = (1 - Z_k^{-1}) D_2^{-1} \quad (42)$$

the closed-loop equations are given by

$$\begin{bmatrix} \dot{x} \\ \dot{x}_k \end{bmatrix} = \begin{bmatrix} A + B_3 Z_k D_k C_3 + B_3 (Z_k - I) D_2^{-1} C_4 & B_3 Z_k C_k \\ B_k C_3 & A_k \end{bmatrix} \times \begin{bmatrix} x \\ x_k \end{bmatrix} + \begin{bmatrix} B_1 + B_3 (Z_k - I) D_2^{-1} D_1 \\ 0_{n_k \times 1} \end{bmatrix} F_s$$

$$z_s = [C_2 \quad 0_{1 \times n_k}] \begin{bmatrix} x \\ x_k \end{bmatrix}.$$

Theorem 6.2: There exists a nonproper, positive real admittance $K(s)$ with $x_k \in \mathbb{R}^{n_k}$ such that $J_5 = \|T_{\hat{F}_s \rightarrow \hat{z}_s}\|_\infty < \gamma$ and A_{cl} is stable, if and only if the following problem is feasible for some $X_{cl} > 0$, $X_k > 0$, $\gamma > 0$ and A_k, B_k, C_k, D_k, Z_k of compatible dimensions:

$$M < 0, \quad \begin{bmatrix} A_k^T X_k + X_k A_k & X_k B_k - C_k^T \\ B_k^T X_k - C_k & -D_k^T - D_k \end{bmatrix} < 0, \quad 0 < Z_k < 1 \quad (43)$$

where $X_{cl} := \begin{bmatrix} X_{11} & X_{12} \\ X_{12}^T & X_{22} \end{bmatrix}$ and M is a symmetric matrix with

$$M_{11} = X_{11} B_3 Z_k D_k C_3 + ()^T + X_{12} B_k C_3 + ()^T + X_{11} B_3 Z_k D_2^{-1} C_4 + ()^T - X_{11} B_3 D_2^{-1} C_4 - ()^T + X_{11} A + ()^T$$

$$M_{12} = X_{11} B_3 Z_k C_k + X_{12} A_k + A^T X_{12} + C_3^T D_k^T Z_k^T B_3^T X_{12} + C_4^T D_2^{-T} Z_k^T B_3^T X_{12} + C_3^T B_k^T X_{22} - C_4^T D_2^{-T} Z_k^T B_3^T X_{12}$$

$$M_{13} = X_{11} B_1 + X_{11} B_3 Z_k D_2^{-1} D_1 - X_{11} B_3 D_2^{-1} D_1$$

$$M_{14} = C_2^T \quad M_{24} = 0_{n_k \times 1} \quad M_{34} = 0$$

$$M_{33} = M_{44} = -\gamma I$$

$$M_{22} = X_{22} A_k + ()^T + X_{12}^T B_3 Z_k C_k + ()^T$$

$$M_{23} = X_{12}^T B_1 + X_{12}^T B_3 Z_k D_2^{-1} D_1 - X_{12}^T B_3 D_2^{-1} D_1.$$

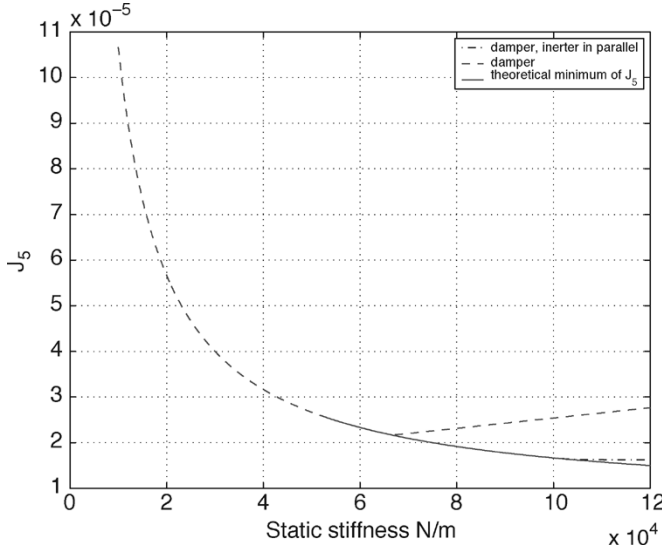


Fig. 15. Optimization results for J_5 over fixed-structure admittances.

The constraint on Z_k ensures that $E_k > 0$ since $D_2^{-1} < 0$. The problem in Theorem 6.2 is also solved locally using a similar iterative algorithm as the one for the proper controller case. The main difference is that the algorithm used updates the controller matrices in two steps rather than in one.

C. J_5 Optimization Results

The proposed algorithms for J_5 optimization will be assessed by comparing the obtained admittances with the fixed-structure admittances suggested in [2]. Fig. 15 presents the optimum J_5 versus static stiffness and shows the extent to which it is achieved by two fixed-structure admittances. The first is a damper, which achieves the optimum up to $k_s = 68$ kN/m and the other is a damper in parallel with an inerter that achieves the optimum up to 102 kN/m.

The algorithm for proper admittances was tested at $k_s = 50$ kN/m. For this value of k_s the optimum is 2.6666×10^{-5} . The algorithm produced a first-order admittance given by

$$K(s) = 6130 + \left(\left(\frac{762}{s} \right)^{-1} + 12591^{-1} \right)^{-1} \quad (44)$$

that guarantees an upper bound of $J_5 < 2.6667 \times 10^{-5}$. The obtained admittance is more complicated than the damper proposed in [2] with optimal setting in the range $6030 \text{ Ns/m} \leq c_{\text{opt}} \leq 19940 \text{ Ns/m}$. An interesting observation is that if we allow the stiffness of the spring in (44) to take its extreme values $(0, \infty)$, then we recover approximately the optimal damper range.

The algorithm for the nonproper admittances was tested for $k_s = 100$ kN/m. For this value of k_s the optimum is 1.6666×10^{-5} . The algorithm produced a first-order admittance given by

$$K(s) = 24010 \frac{0.004}{s + 0.004} + 12008 + 292s \quad (45)$$

that guarantees an upper bound of $J_5 < 1.6667 \times 10^{-5}$. The first-order lag is relatively small so it can be neglected without causing a significant degradation in J_5 . Thus, the suspension

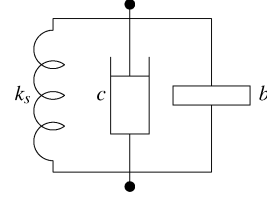


Fig. 16. Quarter-car suspension as a parallel connection of a spring, a damper, and an inerter.

consists of a parallel connection of a spring $k_s = 100$ kN/m, a damper $c = 12008$ Ns/m, and an inerter $b = 292$ kg (Fig. 16). The optimal suspension proposed in [2] for this value of k_s is in fact a damper in parallel with an inerter with optimal values in the ranges

$$11\,380 \text{ Ns/m} \leq c_{\text{opt}} \leq 12\,287 \text{ Ns/m} \quad 269 \text{ kg} \leq b_{\text{opt}} \leq 337 \text{ kg}.$$

The suspension obtained by the LMI optimization is within the above range. Moreover the LMI algorithm managed to find a second-order suspension that achieves the theoretical minimum at the top range of k_s , which could not be achieved with the fixed-order admittances considered in [2]. The resulting admittance was given by

$$K(s) = 51\,450 \frac{s^2 + 14.11s + 1302}{s^2 + 67.66s + 4468} + 423s \quad (46)$$

which gave a rather complicated network when using the Bott–Duffin realization method [16]. The existence of a simpler realization is currently being investigated.

VII. MULTI-OBJECTIVE OPTIMIZATION AND OTHER GENERALIZATIONS

The practical design of vehicle suspension systems usually involves a tradeoff between a variety of performance objectives [2], [4]. It is possible to extend the techniques of the present paper to include multi-objective optimization. To illustrate this, we consider the case of the combined optimization of the measures J_1 and J_3 defined above. The approach taken here is to minimize

$$\sqrt{(1-\lambda) \frac{J_1^2}{\hat{J}_1^2} + \lambda \frac{J_3^2}{\hat{J}_3^2}} \quad (47)$$

for $0 < \lambda < 1$, where \hat{J}_1 and \hat{J}_3 are the optimal values obtained in the single-objective optimizations. To solve this problem, a generalized plant was formulated with the two performance outputs being the appropriate scalar multiples of \dot{z}_s and $\int(z_u - z_r)$. A new theorem was written down which is directly analogous to Theorem 4.1 to give a necessary and sufficient condition for the achievement of a certain performance level. This characterization was again in the form of an BMI which was solved using the iterative algorithm implemented in YALMIP. This problem was solved for a range of λ values in the interval $(0,1)$ with a fixed static stiffness $k_s = 60$ kN/m. The results obtained are shown in Fig. 17.

The LMI formulation of the positive real synthesis problem allows the flexibility for further generalization. For example, the issue of model uncertainty can be included. One approach is to

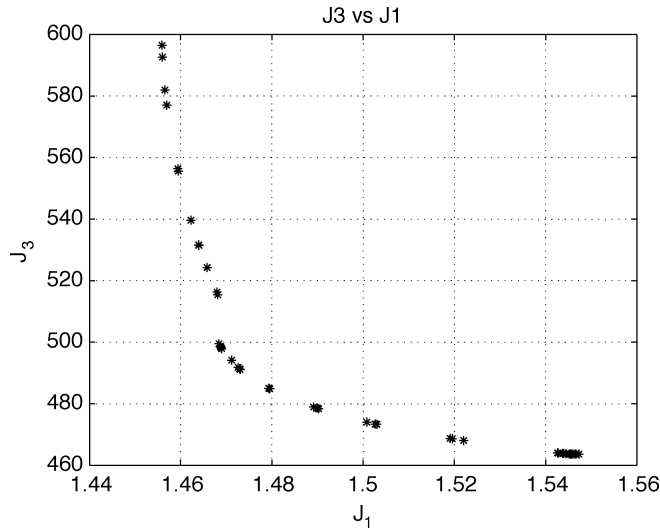


Fig. 17. Multi-objective optimization of J_1 and J_3 .

use a multi-model formulation for a discrete set of parameter values. Alternatively, an LFT formulation can be used for an appropriate choice of uncertain real parameters (see [17, Lemma 3]). Optimization results were obtained for the latter approach using the uncertain parameters m_s and k_t , but these are not included for reasons of space.

VIII. EXPERIMENTAL TESTING OF A MECHANICAL NETWORK INVOLVING AN INERTER

A mechanical network comprising an inerter in series with a parallel combination of a spring and a damper was designed and built at CUED. Experimental testing of the network was carried out using the Schenck Hydraulic Test Rig shown in Fig. 18. In this setup, the displacement of the hydraulic ram can be controlled and it is possible to apply reference sinusoidal signals of different frequencies and amplitudes from a MATLAB/Simulink environment that interfaces with a DSpace processor. There also exists a load cell that measures the force through the load specimen, thus, making possible the calculation of the load admittance.

The inerter device used in the mechanical network is of a ball-screw type and was designed and built in the workshops of CUED. A picture of the device, partially disassembled, is shown in Fig. 19. The inertance of the device is achieved by the rotation of the nut to which a flywheel is attached. Inertances of 50, 130, and 230 kg can be realized by using different flywheels (according to the analysis carried out on the experimental data [18]), while the actual mass of the device is about 1 kg. A displacement sensor (LVDT) is placed across the inerter so that a calculation of the inerter admittance is possible. A high-performance damper, typical of racing car applications, is used in the network with a damper rate of 4 kNs/m. The spring effect is produced through the use of a titanium spring cantilever which is supported by an L-shaped aluminium frame. The spring rate was calculated as 250 kN/m. The whole load arrangement is excited at its lower end by the hydraulic ram, with the load cell located at the fixed top end of the load specimen. The particular

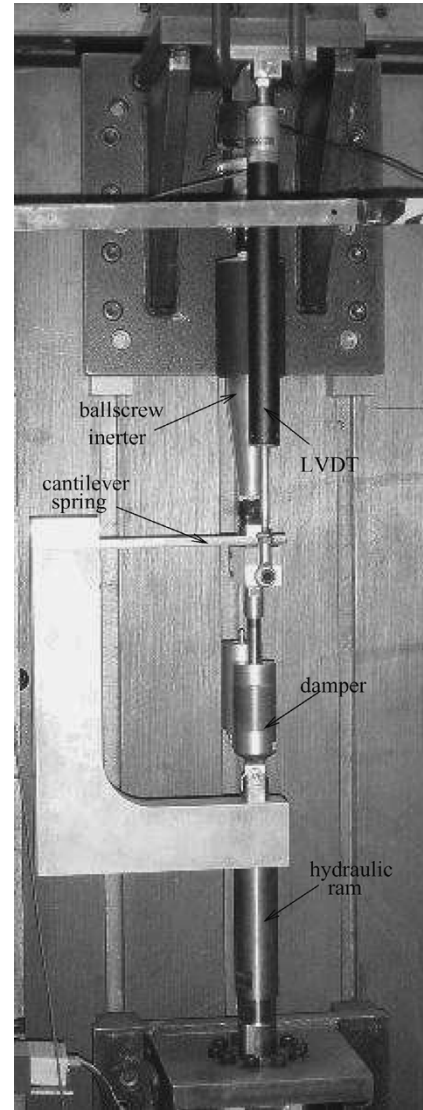


Fig. 18. Mechanical network on the hydraulic test rig.

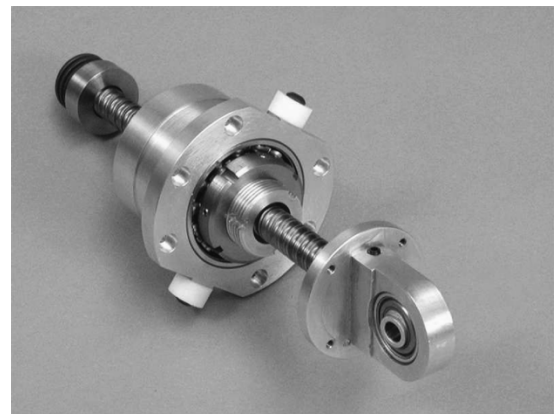


Fig. 19. Ball-screw inerter made at CUED with cover and flywheel removed.

network tested was chosen so that its admittance behaves approximately like a damper at high frequencies (see Fig. 13), and more specifically, around the crossover frequency of the rig's control system. The benefit of this choice is that no adjustment of the control system was anticipated from its normal settings

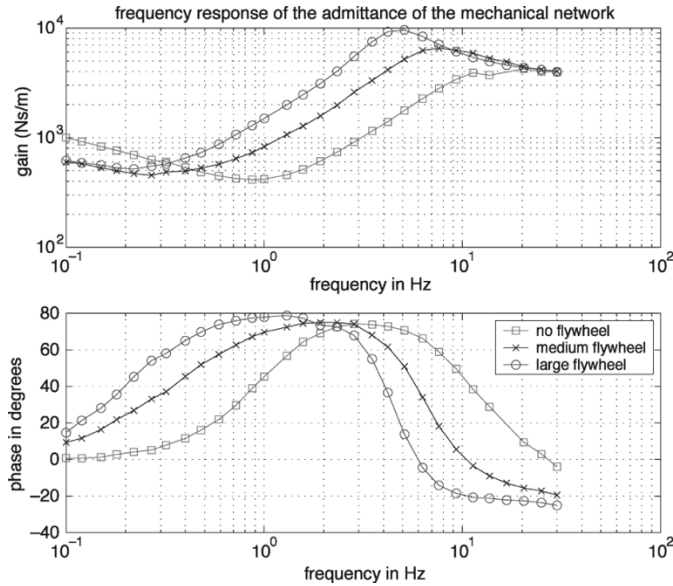


Fig. 20. Admittance of the mechanical network calculated from experimental testing.

used for testing dampers. It was known that other admittance behaviors could lead to instability, but this was not experienced in the present case.

The calculation of the admittance of both the inerter and the whole load was achieved by applying sinusoidal excitation signals in the frequency range of 0.1–30 Hz, and recording the relevant signals which are the ram displacement, the inerter displacement, and the load force. At each frequency point, the gain and phase of the admittance of the load and the inerter were calculated using the correlation method described in [18]. The results are presented in Fig. 20 for three cases: with no flywheel in the inerter, with the medium flywheel, and with the large flywheel.

The theoretical admittance of such a network is given by

$$Y(s) = bs \left(\frac{\frac{k}{b}}{s^2 + \left(\frac{c}{b}\right)s + \frac{k}{b}} \right) \left(1 + \left(\frac{c}{k}\right)s \right) \quad (48)$$

where b is the inertance, c is the damper rate, and k is the spring rate. The second-order system has a natural frequency of $\sqrt{k/b}$ rad/s and a damping factor of $c/(2\sqrt{bk})$. Furthermore, we have $\lim_{s \rightarrow \infty} Y(s) = c$ and $\lim_{s \rightarrow 0} Y(s)/s = b$, so that the theoretical network behaves like a damper at high frequencies and like an inerter at low frequencies. We see from Fig. 20 that at high frequencies the network indeed behaves like a damper of approximately 4-kNs/m and this is independent of the inertance value. In all three cases, there is an intermediate frequency range in which the experimental admittance tends toward the inerter admittance bs and we get a considerable phase advance. As the flywheel inertance increases, the observed natural frequency indeed becomes smaller, and lighter damping is evident. The experimental results match the theoretical model of the admittance apart from the case when the frequency tends to zero. Interestingly, the experimental results at low frequencies are inconsistent with linear theory, since the phase tends to zero while the gain shows an increase of approximately 10 dB/dec. It is expected that the low-frequency behavior is influenced by friction

in the inerter device, although, more investigation is required in order to model these effects.

IX. CONCLUSION

The problem with synthesis of positive real controllers was formulated using matrix inequalities. Two local optimization methods were proposed to solve the bilinear matrix inequality problems in the context of suspension design for a quarter-car vehicle model. The algorithms were successful in obtaining previously found solutions when optimizing over fixed-structure admittances. In the case of the performance measure J_1 , which characterizes the response of the sprung mass due to road disturbances, the proposed algorithm found alternative admittances that improve the performance measure considerably. In the case of the performance measure J_3 , which characterizes the tyre normal load, the network realizations of the admittances from the optimization were shown to be relatively simple and implementable networks. In the case of the performance measure J_5 , which characterizes the effect of dynamic loads on the sprung mass, the algorithm found positive real admittances which achieved a theoretical lower bound at high-static stiffness values, which previously had only been achieved at lower stiffnesses. A prototype inerter was built and tested at CUED in a mechanical network comprising one inerter, one damper, and one spring. The measured frequency responses gave a good match to the theoretical predictions over the frequency range 0.5 Hz–30 Hz.

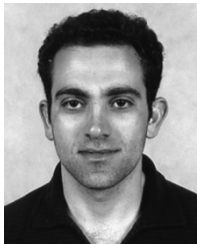
ACKNOWLEDGMENT

The authors are most grateful to N. Houghton, J. Beavis, B. Puddifoot, and A. Ross for their work in the design and manufacture of the inerter prototype. They would also like to thank D. Cebon for making the Vehicle Dynamics Group's hydraulic ram available to them, and R. Roebuck for his assistance in the experiments.

REFERENCES

- [1] M. C. Smith, "Synthesis of mechanical networks: The inerter," *IEEE Trans. Autom. Control*, vol. 47, no. 10, pp. 1648–1662, Oct. 2002.
- [2] M. C. Smith and F.-C. Wang, "Performance benefits in passive vehicle suspensions employing inerters," *Veh. Syst. Dynamics*, vol. 42, no. 4, p. 235, 2004.
- [3] S. Boyd, L. El Ghaoui, E. Feron, and B. Balakrishnan, *Linear Matrix Inequalities in System and Control Theory*. Philadelphia, PA: SIAM, 1994.
- [4] J. Wang and D. A. Wilson, "Mixed $GL_2/H_2/GH_2$ control with pole placement and its application to vehicle active suspension systems," *Int. J. Control*, vol. 74, no. 13, pp. 1353–1369, 2001.
- [5] J. C. Geromel and P. B. Gapski, "Synthesis of positive real H_2 controllers," in *Proc. Conf. Decision Control*, Kobe, Japan, 1996, pp. 2864–2869.
- [6] T. Shimomura, Y. Yamasaki, and T. Fujii, "LMI-based iterative synthesis of strictly positive real H_2 controllers," in *Proc. Amer. Control Conf.*, Chicago, IL, 2001, pp. 332–336.
- [7] J. L. Shearer, A. T. Murphy, and H. H. Richardson, *Introduction to System Dynamics*. Reading, MA: Addison-Wesley, 1967.
- [8] R. W. Newcomb, *Linear Multiport Synthesis*. New York: McGraw-Hill, 1966.
- [9] O. Brune, "Synthesis of a finite two-terminal network whose driving-point impedance is a prescribed function of frequency," *J. Math. Phys.*, vol. 10, pp. 191–236, 1931.
- [10] R. Bott and R. J. Duffin, "Impedance synthesis without use of transformers," *J. Appl. Phys.*, vol. 20, p. 816, 1949.

- [11] K. Zhou, C. J. Doyle, and K. Glover, *Robust and Optimal Control*. Englewood Cliffs, NJ: Prentice-Hall, 1996.
- [12] C. Scherer, P. Gahinet, and M. Chilali, "Multi-objective output-feedback control via LMI optimization," *IEEE Trans. Autom. Control*, vol. 42, no. 7, pp. 896–911, Jul. 1997.
- [13] A. Hassibi, J. How, and S. Boyd, "A path-following method for solving BMI problems in control," in *Proc. Amer. Control Conf.*, San Diego, CA, 1999, pp. 1385–1389.
- [14] J. Löfberg, (2004) YALMIP 3. [Online]. Available: <http://control.ee.ethz.ch/joloeff/yalmip.msql>.
- [15] P. Gahinet and P. Apkarian, "A linear matrix inequality approach to H_∞ control," *Int. J. Robust Nonlinear Control*, vol. 4, pp. 421–448, 1999.
- [16] E. A. Guillemin, *Synthesis of Passive Networks*. New York: Wiley, 1957.
- [17] K. Sun and A. Packard, "Robust H_2 and H_∞ filters for uncertain LFT systems," *IEEE Trans. Autom. Control*, vol. 50, no. 5, pp. 715–720, May 2005.
- [18] C. Papageorgiou, "Experimental testing of inerter devices," CUED, Cambridge, U.K., Tech. Rep. CUED/F-INFENG/TR.504, Dec. 2004.



Christakis Papageorgiou received the B.A. (M.Eng.) degree in electrical and information sciences, and the Ph.D. degree in control systems from Cambridge University, Cambridge, U.K., in 1999 and 2003, respectively.

His main subject of study was the application of nonlinear control design techniques for the control of aeroservoelastic aircraft. He worked in the Control Lab as a Research Associate at the University of Cambridge, until 2004, where he carried-out research on a novel mechanical element, the inerter. Between

January 2005 and January 2006, he was a Research Associate in the Department of Electrical and Computer Engineering at the University of Cyprus, Nicosia, Cyprus, working on a project in collaboration with the Engineering Department at the University of Cambridge, which was partially funded by the Research Promotion Foundation in Cyprus. His research interests include robust and optimal control with linear matrix inequalities, analysis and design of control laws for aeroservoelastic systems, vibration suppression and rejection of structural vibrations, robustness analysis of nonlinear flight control laws and synthesis, and experimental testing of passive mechanical networks for vehicle suspensions.



Malcolm C. Smith (M'90–SM'00–F'02) received the B.A. (M.A.) degree in mathematics in 1978, the M.Phil. degree in control engineering and operational research in 1979, and the Ph.D. degree in control engineering in 1982, all from Cambridge University, Cambridge, U.K.

He was subsequently a Research Fellow at the German Aerospace Center, Oberpfaffenhofen, a Visiting Assistant Professor and Research Fellow with the Department of Electrical Engineering at McGill University, Montreal, QC, Canada, and

an Assistant Professor with the Department of Electrical Engineering at the Ohio State University, Columbus, OH. In 1990, he joined the Engineering Department at the University of Cambridge, where he is currently a Professor. His research interests are in the areas of robust control, nonlinear systems, and automotive applications.

Dr. Smith is a co-recipient with Dr. T. T. Georgiou of the 1992 and 1999 George Axelby Best Paper Awards, in the IEEE TRANSACTIONS ON AUTOMATIC CONTROL.